

Article ID: 1006-8775(2010) 02-0160-11

THE ROLE OF COLD AIR AND CHARACTERISTICS OF WATER VAPOR IN BOTH TCS NANMADOL (0428) AND IRMA (7427) MAKING LANDFALL ON CHINA IN WINTERTIME

HE Jie-lin (何洁琳)^{1,2}, GUAN Zhao-yong (管兆勇)¹, WAN Qi-lin (万齐林)³, WANG Li-juan (王黎娟)¹

(1. KLME, Nanjing University of Information Science & Technology, Nanjing 210044 China; 2. Yulin City Meteorological Bureau of Guangxi, Yulin 537000 China; 3. Guangzhou Institute of Tropical and Marine Meteorology, CMA, Guangzhou 510080 China)

Abstract: The NCEP/NCAR reanalysis data are used to investigate the role of cold air and moisture characteristics during the evolution of two cases of tropical cyclones (Nanmadol and Irma) which made landfall on China in wintertime. The results are shown as follows. (1) The East Asia trough steered the cold air into the tropical ocean in early winter. The tropical cyclones moved in opposite directions with a high moving out to sea and the enhancement of the pressure gradient at the periphery played a role in maintaining and strengthening the intensity of the storms. The intrusion of weak cold air into the low levels of the tropical cyclones strengthened them by improving the cyclonic disturbance when they were still over the warm sea surface. When the cold air was strong enough and intruded into the eyes, the warm cores were damaged and stuffed before dissipation. (2) The tropical cyclones were formed in a convergence zone of moisture flux and their development could enhance the disturbance of water vapor convergence, thus strengthening the moisture convergence zone. However, when they were outside the moisture zone, the storms could not gain sufficient water vapor and became weak. There were no belts of strong moisture transportation during the wintertime tropical cyclone processes.

Key words: tropical cyclones, cold air, water vapor, wintertime

CLC number: P444

Document code: A

doi: 10.3969/j.issn.1006-8775.2010.02.008

1 INTRODUCTION

China is one of the countries which are seriously affected by tropical cyclones (TCs). One of the current focuses of research on meteorological disasters is the landfalling TCs. While TCs generally make landfall in summertime, it is extremely rare for them to land on China in wintertime. The statistics^[1-3] revealed that there are only two wintertime TCs that made landfall in China since 1949, among which Irma landed in Taishan, Guangdong province, on December 2, 1974 and Nanmadol landed in the island of Taiwan on December 4, 2004. As there are few occurrences of landfalling TCs in wintertime, little attention is paid to the studies of wintertime TCs. The cold air can affect the genesis and development of TCs in autumn and winter. Chen et al. summarized previous studies about the possible mechanism of cold surges on the genesis

and development of TCs, which are presented as follows: The pressure gradient increases at the periphery of TC; cold air intrusion improves the role of the Convective Instability of the Second Kind (CISK); the horizontal temperature gradient occurs when the cold air reaches a certain latitude, which plays a role in enhancing the cyclonic vorticity; a large region of the convective clouds occur when the cold air reaches the tropics, which provides suitable environments for the development of the tropical disturbances. The establishment and strengthening of the cold-air-related wintertime monsoon also play an important role in the genesis and development of TCs^[4]. On the other hand, water vapor transportation is an important factor in the genesis and development of TCs. A large number of moist air is involved in the TC due to the southwesterly low-level jet, which releases the latent heat to maintain

Received date: 2009-11-18; **revised date:** 2010-01-16

Foundation item: National Development and Plan for Key Fundamental Research (2009CB421505); 11th National Five-Year Plan for Science Support (2006BAC02B); National Natural Science Foundation (40775058); Natural Science Foundation of Guangxi (2010GXNSFA013010)

Biography: HE Jie-lin, Ph.D. candidate, mainly undertaking the research on monsoon dynamics.
E-mail for corresponding author: hjlchinese@163.com

the development of TC [5-7]. After landfall, the water vapor from the south contributes much to the maintenance of TC [8]. The characteristics and abrupt change of the track of Nanmadol have been studied [9-10], but no comprehensive analysis of the two landfalling wintertime TCs have been done, and no detailed study on the role of cold air and water vapor has been undertaken. Thus, the present paper will mainly work on them.

2 DATA AND METHODS

The observations of the TCs are obtained from Tropical Cyclone Yearbook which is published by China Meteorological Press [3, 11]. The NCEP/NCAR reanalysis data that are available 4 times daily are used [12]. The role of cold air in TCs is explored in aspects such as the large-scale circulation, the relationship between cold air and TC intensity, and the thermal structure of TC. The features of water vapor in the process of TCs are analyzed by using the velocity potential function and divergent wind of the whole-layer moisture flux, and the low-level moisture flux are taken into account, too.

The solving method for the velocity potential function [13] and the calculation steps of the moisture flux and the divergence variable [14] are as follows: The water vapor flux \vec{Q} and divergence component are calculated according to the values of q , u , and v on every grid in the whole field; Then the potential function of water vapor flux χ is calculated by resolving the Poisson equation $\nabla^2 \chi = -\nabla \cdot \vec{Q}$. Next, the net χ' is integrated vertically from the surface to 300 hPa and the divergence component $\vec{Q}_{\chi'} = -\nabla \chi'$ of the whole-layer moisture per unit area is attained in the end.

3 OVERVIEW OF TCS NANMADOL AND IRMA

Figure 1 shows the tracks of Nanmadol and Irma. Having been generated at 153.7°E, 5.7°N on the western North Pacific (WNP) on November 28 in 2004, Nanmadol, then a tropical depression, reached a minimum pressure of 950 hPa and maximum wind speed of 45 m/s near the center during the whole lifecycle. It then moved to the northwest, made its first landfall on Luzon of the Philippines and went ahead and turned to the northeast and made its second landfall on Taiwan Island on the morning of December 4. Only two to three hours on land, it quickly moved into the ocean again, weakened and disappeared. Having been formed at 140.2°E, 10.3°N in the WNP on November

22, 1974, TC Irma had a central minimum pressure of 939 hPa and maximum wind speed of 50 m/s during the process. Like TC Nanmadol, it landed on Luzon first and then went on to the mainland, turned to make the second landfall on Taishan, Guangdong, in the south of China, and soon weakened to dissipate.

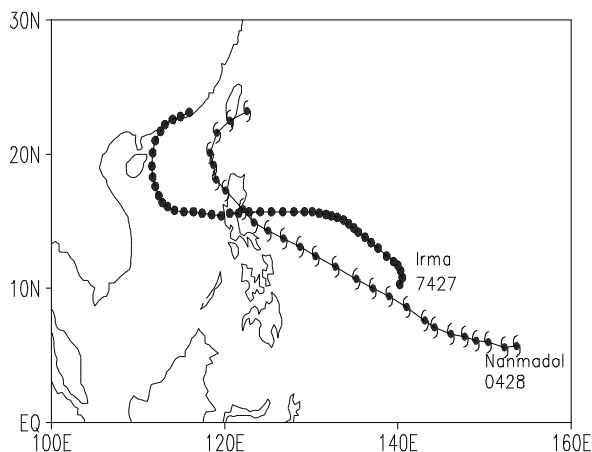


Fig.1 Paths of Nanmadol (line with a typhoon symbol) and Irma (dotted line).

4 ROLE OF COLD AIR

4.1 Basic large-scale circulation

Previous studies have found that a surface northeast flow enhanced after the occurrence of cold surges during the East Asia wintertime monsoon period, which strengthened the convection near the Equator [15, 16]. Sun et al. [17] pointed out that a deepened trough over East Asia in winter can significantly enhance the tropical convective activity at 110°E–150°E and north of the Equator, and the wintertime wind can stimulate the activities of the tropical convection. Figure 2 shows the mean thermal advection and wind vector fields on the 1000-hPa level of the two TCs' processes. It can be seen that in both the processes, the northeast wind dominates the tropical WNP region, the cold advection areas are mainly in the ocean in which strong cold advection is located in the vicinity of Japan, just behind a major trough over East Asia and the anti-cyclone center is located at about 40°N, 130°E. The strong low-level northwest flow in mid-high latitudes makes recurvature at about 30°N so that the weak cold advection can reach the tropical WNP and South China Sea (SCS) to increase the northeast wind speed. The cold surge can reach the 5°N to 20°N tropical oceans. Thus, the East Asian trough introduces the weak cold air to the tropical oceans frequently during the two processes, favoring the development of tropical convection.

4.2 Relationship between the cold air and the intensity of TC

Previous studies [18 - 20] have pointed out that, in general, the convective cloud amounts increased when the cold surge occurred in tropical oceans, and so did the cyclonic vortices at 850 hPa, and thus the organized deep convections grew and led to the development of the already existing cyclonic vortex disturbances. Therefore, the large-scale circulation which was in favor of cold air to reach the tropical ocean plays an important role in the formation and development of TCs. The cold air process here refers to the continental high moving out to the ocean and influencing the TC's periphery and the activities of TCs over the ocean are mainly considered. The whole process of Irma began at the time when it was officially coded at 0800 November 29 (Beijing time, the same below) and ended at 1400 December 4. Observations are available once every 6 h and there are a total of 22 times of observations. Irma was covered from a time of its generation at 0800 November 22 to that right before its landfall on Taishan, with a total of 41 times of observations. To quantify the impact of cold air on TC intensity, a cold air index $SLPP$ is defined based on the positive correlation between the intensity of cold air and the pressure gradient, as well as the analysis of the large-scale circulation in the TCs processes. The detailed definition is as follows.

The time series $\{slp_i = p_{40_i} - p_{25_i}\}$ indicates that the cold air intensity that reaches the periphery of the TC, in which p_{40_i} and p_{25_i} refer to the 110°E to 140°E zonal mean of sea level pressure along 40°N and 25°N, respectively. Here p_{40_i} indicates the intensity of the high pressure moving into the sea and p_{25_i} indicates the pressure outside the TCs. Then the standardized series $\{slpp_i\}$ is the cold air index, namely $SLPP = \{slpp_i\}$. The values of $SLPP$ correlate positively to the intensity of cold air which affects the TCs.

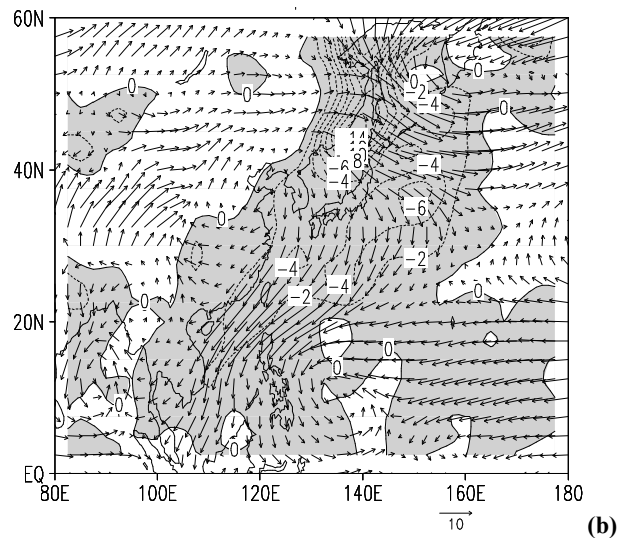
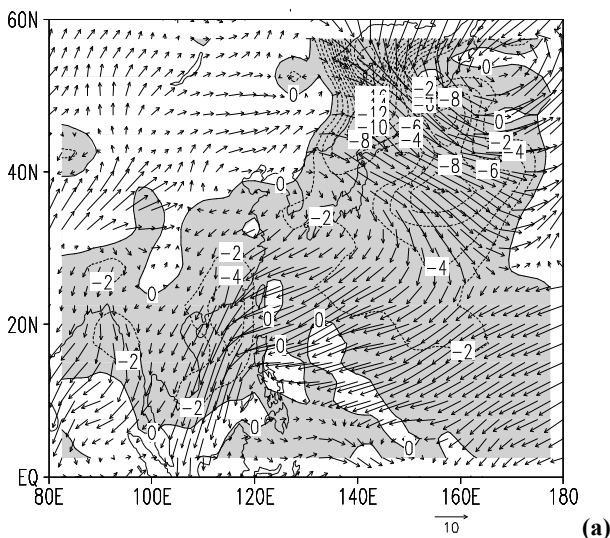


Fig.2 Mean temperature advection and wind fields at 1000 hPa during the TCs processes. a: Nanmadol, averaged from November 28 to December 4, 2004; b: Irma, averaged from November 22 to December 3, 1974. Shades and dashed contours are negative temperature advctions, units are $1 \times 10^{-5} \text{ }^\circ\text{C/s}$, intervals are 2 and vectors are for the wind field in the unit of m/s, and the vector length denotes the values of wind speed.

The index PP is defined as the intensity of the TC. The time series $\{pty_i\}$ is the minimum center pressure in a TC process. Then the series $\{pty_i\}$ is standardized to determine a time series $\{pp_i\}$ as the TC intensity index, namely $PP = \{pp_i\}$. The smaller the value of PP , the greater the intensity of the TC. $i = 1, 2, \dots, n$. For all of the above defined indexes, where n is the observed times of the whole lifecycle of a TC, n is 22 and 41 for Nanmadol and Irma, respectively.

The index series of $\{slpp_i\}$, $\{pp_i\}$ and $\{p_{40_i}\}$, $\{p_{25_i}\}$ for Nanmadol and Irma were plotted (Fig. 3). $\{p_{40_i}\}$ and $\{p_{25_i}\}$ were processed before plotting in order to be displayed in the same coordinates. It can be seen that the larger the value of p_{40_i} the larger that of $slpp_i$, and the variations of p_{25_i} coincide with those of p_{40_i} , so the index $SLPP$ indicates the strength of cold air at the TC periphery. On the other hand, the variations of pp_i are contrary to those of p_{40_i} and $slpp_i$; the larger the values of p_{40_i} and $slpp_i$ the smaller that of pp_i , which indicates the relationship between the cold air and the intensity of the TC: the stronger the high moving out to sea and the pressure gradient outside the TC, the stronger the TC. The trough of the curve of $\{pp_i\}$ in Fig. 3a denotes the strongest intensity of Nanmadol for its mature stage, while the peaks in both the head and tail of the curve denote the weak intensity in the period of TC genesis

and decay, and the peaks in the curve of $\{slpp_i\}$ denote the large north-south pressure gradient over 110°E to 140°E . It can be easily seen that the trough values of series $\{pp_i\}$ during the period of the matured TC coincide with the peak values of $\{slpp_i\}$. In the sea level pressure fields from 2000 November 30 to 0800 December 2 ($i = 7$ to 13), there was a process in which a cold high whose the center intensity was greater than 1037.5 hPa was moving to the sea from the Shandong Peninsula and the TC was moving towards it at the same time. In Fig. 3b, there are two peaks in the curve of $\{slpp_i\}$ of the lifecycle of Irma, of which the first peak ($i = 12$ to 21) corresponds to the cold air process from November 24 to 27, and the second peak ($i = 30$ to 36) reflects the process from November 29 to 30, with the intensity of cold high pressure greater than 1025 hPa. Accordingly, the two troughs in the curve of $\{pp_i\}$ coincide with the two peaks of $\{slpp_i\}$. The corresponding sea-level pressure fields of the three cold air processes for the time of the strongest intensity are shown in Fig. 4, which indicates the presence of an enhanced pressure gradient at the northern periphery of the TC. The correlation coefficients between the series $\{slpp_i\}$ and $\{pp_i\}$ for Nanmadol and Irma are -0.87 and -0.44 , respectively, both being significant at the 99.9% confidence level. There is a remarkable negative correlation between the cold air index and the intensity of TC during the two processes, which indicates that the larger the value of the cold air index the stronger the TC.

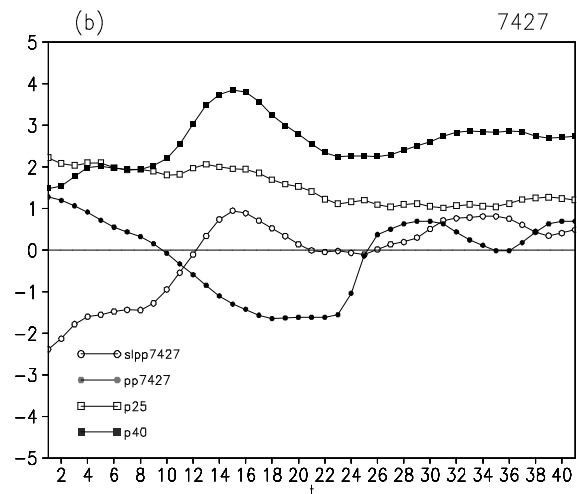
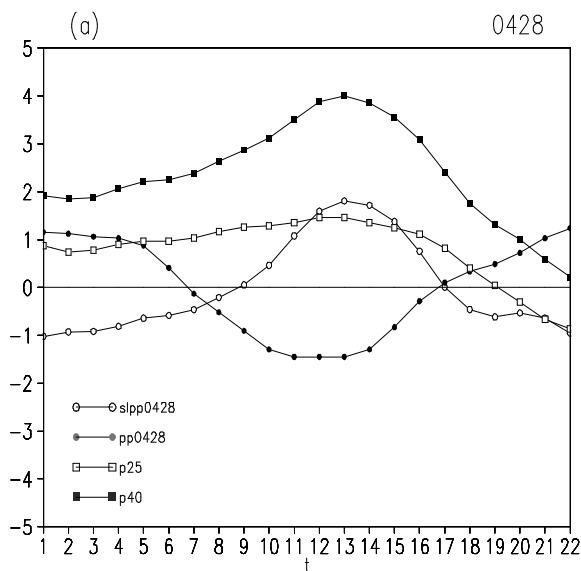


Fig.3 Time series of cold air index $SLPP$ (hollow-circle line) and TC intensity index PP (solid-dotted line) during the process of Nanmadol (a) and Irma (b). Lines with solid and hollow boxes represent p_{40} and p_{25} , respectively (original value minus 1015 or 1008, then divided by 5). The abscissa unit is the order of times.

Previous studies have suggested that the cold air in the fall and winter seasons could enhance pressure at the periphery of TCs so that the wind speed on the north side of the TC increased and there were corresponding increases in cyclonic vorticity which contributed to the development and strengthening of TCs^[4]. In the present article, the analysis of the two wintertime TC processes also shows that when a moderate-intensity cold high over mid-high latitudes moves out from northeastern China to the sea and a TC moves towards the same region, the pressure gradient outside of the TC increases and the TC also intensifies.

4.3 Cold air reflection in the TC warm core structure

The role of cold air in the TCs is explored by analyzing their thermal structure in this section. The observations at 0800 December 2 and 0800 December 4 are selected as the represented times for the mature and weakening stages of Nanmadol, respectively. The TC is mature and stable at 0800 December 2 (Fig. 4a) while the continental cold high moves out to sea across the northern Korean Peninsula, with the high center located north of the TC at about 40°N , 130°E , i.e., the greatest pressure gradient is outside of the TC. At this point in the 1000-hPa temperature advection and wind field (Fig. 5a), weak cold advection caused by the northeast flow reaches the west side of the TC. Figure 5b shows the corresponding temperature deviation of the vertical cross section passing across the TC center, which has the characteristics of a warm core typical of a matured TC. The warm core is at 300 to 200 hPa and temperature is 5°C higher than that around it, with a

+3°C warm core located on the 850-hPa level. A small region of negative temperature deviation—which is less than -1°C at 1000 to 900 hPa—is located on the west side of the external part of the TC, indicating a weak cold air at the periphery. Nanmadol weakened before landfalling on the island of Taiwan at 0800 December 4. It can be seen in the daily circulation fields (figures not shown) that another strong continental cold high moved into the south of China at this time and the northwest flow steered by an 500-hPa upper trough controls the mainland. It is also shown in the temperature advection and wind fields on the 1000-hPa level (Fig. 5c) that a strong cold advection zone induced by the northwest airflow is located on the

west side of the TC with the center values greater than $18 \times 10^{-5} \text{ } ^\circ\text{C/s}$. In the cross section corresponding to the vertical temperature deviation (Fig. 5d), the negative temperature deviations from low levels through the 500-hPa level intrude into the center of the TC, with the smallest value of negative temperature deviation less than -5°C. The high-level warm core departs from the center of the TC and the low-level warm core no longer exists. It then suggested that the mid- and low-level cold air penetrates into the TC and destructs and stuffs the warm core. In the end, the cold air caused the decay of Nanmadol.

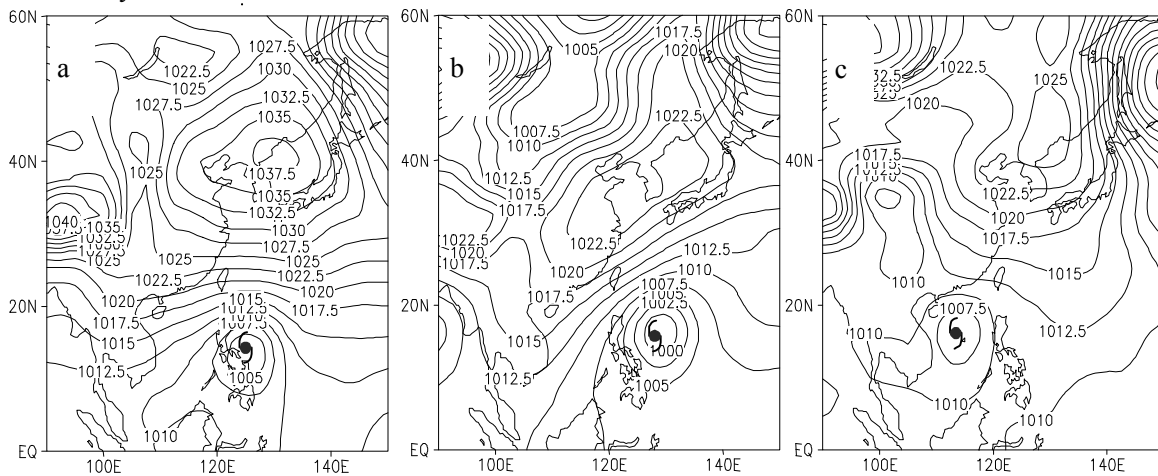


Fig.4 Sea-level pressure fields during the cold air processes. a: 0800 Dec. 2, 2004; b: 0200 Nov. 27, 1974; c: 0800 Nov. 30, 1974. Unit: hPa. The typhoon symbol denotes the position of the TC center.

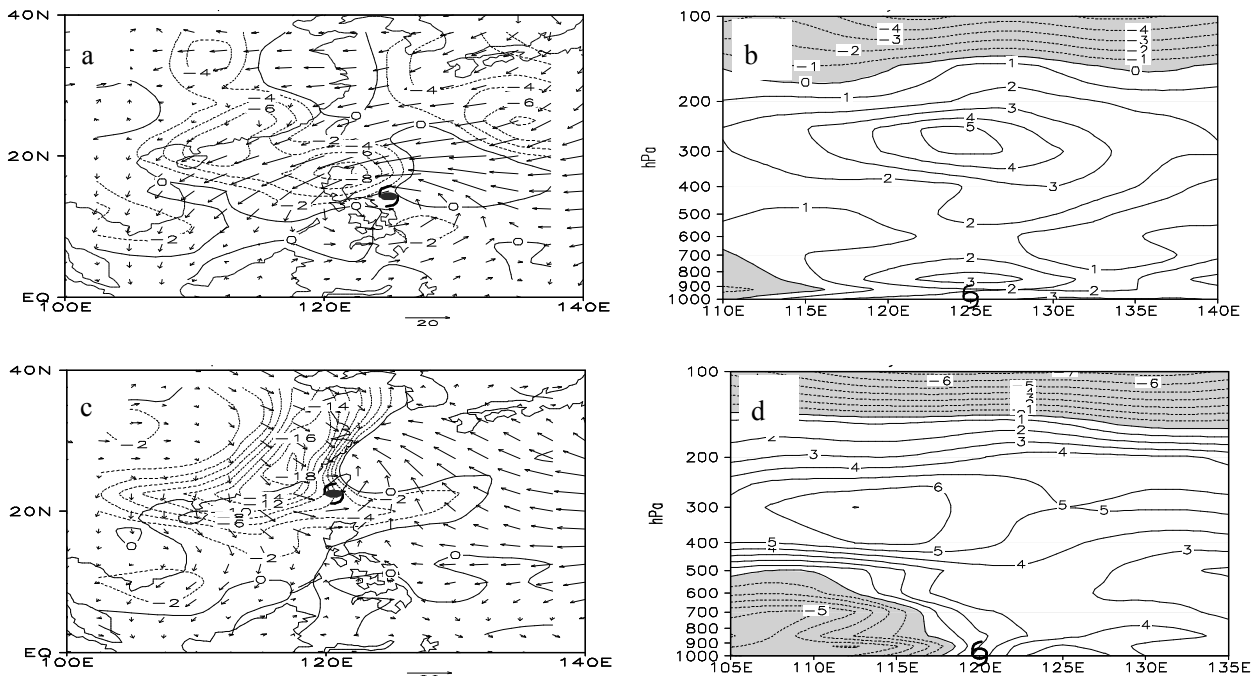


Fig.5 1000-hPa temperature advection and wind (left) and cross sections of temperature zonal deviation along the TC center (right) at 0800 December 2 (above) and 0800 December 4 (below). The dashed (solid) contours are negative (positive) temperature advctions, intervals are $2 \times 10^{-5} \text{ } ^\circ\text{C/s}$, vectors are winds in (a) and (c); the dashed (solid) contours are negative (positive) temperature zonal deviations, intervals are $1 \text{ } ^\circ\text{C}$, and shades are negative in (b) and (d); the typhoon symbol denotes the position of the TC center.

The observations of 0200 November 27 and 0800 November 30 in the process of Irma are selected for analysis, corresponding to the two previously mentioned cold air processes from November 24 to 27, and from November 29 to 30 (Figure 4b & 4c). Figure 6a shows the variables at 0200 November 27 when the TC was mature and stable. Due to the cold air, the negative temperature advection caused by northeast airflows is located on the west side of the TC. At the same time a clear warm core with values higher than $+5^{\circ}\text{C}$ is located at 300 hPa in the vertical cross-section (Fig. 6b), and a region of negative temperature deviation lower than -4°C is located on the west side of the TC below the 700-hPa level, while the values of -1°C only reach the storm's periphery, indicating that the weak cold air gets as far as the periphery of Irma.

There are also weak cold advection west of Irma at 0800 on November 30 (Fig. 6c), and the corresponding vertical cross section (Fig. 6d) shows negative anomalies on the west side of the TC center at levels lower than 900 hPa, indicating that the low-level cold air has penetrated into the TC. Though the TC was still over the SCS at that time, its corresponding intensity was strengthened rather than weakened and the center pressure decreased by 5 hPa and wind velocity increased by 5 m/s as compared with those of the previous observation times. In the circumstances that the water vapor, heat and other conditions remain sufficient, the shallow cold air intruded into the TC and increased the baroclinicity so that the vorticity of the TC increased. The intrusion of low-level cold air has played a stimulating role in strengthening the TC.

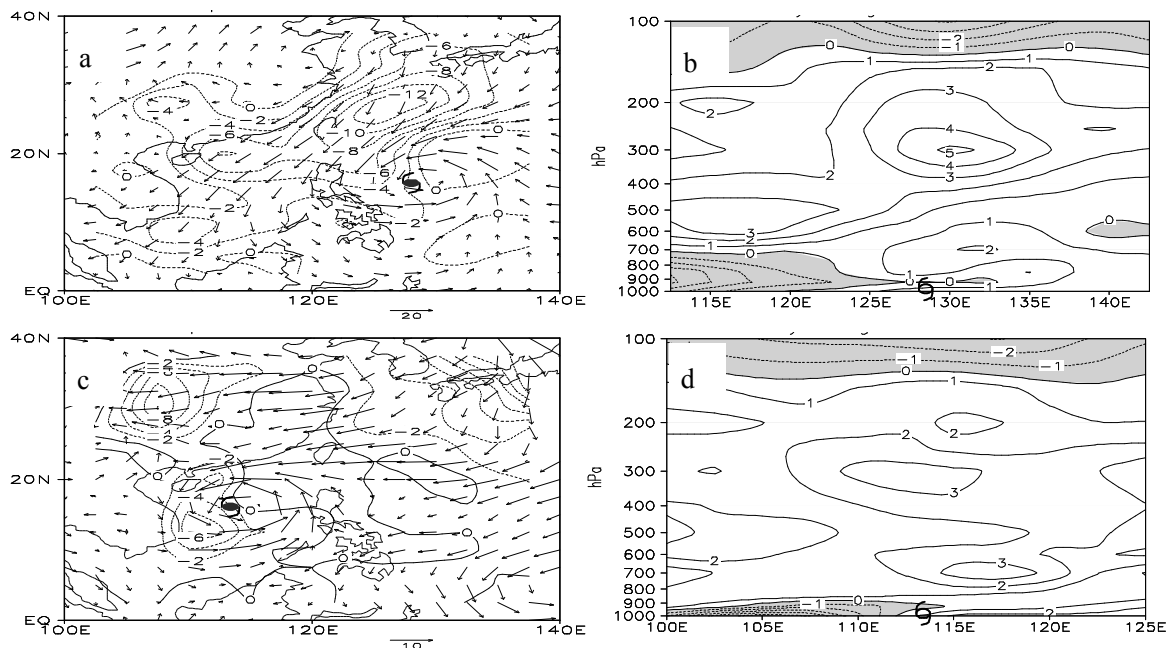


Fig.6 1000-hPa temperature advection and wind (a, c) and cross sections of temperature zonal deviation along the TC center (b, d) at 0200 November 27 (above) and 0800 November 30 (below) of Irma. The captions of variables are the same as Fig. 5.

From all of the above analysis, it is indicated that under the favorable early-winter conditions, large-scale wintertime circulation channels the northern cold surge to the tropical ocean and contributes to the formation and development of TCs; the TCs and the cold high move to meet each other, the increasing external pressure gradient plays a role in maintaining and strengthening the TC intensity; The intrusion of weak low-level cold air into the TC which is still over the warm sea can enhance the vorticity and strengthen the TC. On the other hand, when the cold air intrudes into the middle level of the TC, the warm core could be destroyed and the TC is stuffed in decay.

5 LARGE-SCALE CHARACTERISTICS OF WATER VAPOR TRANSPORTATION

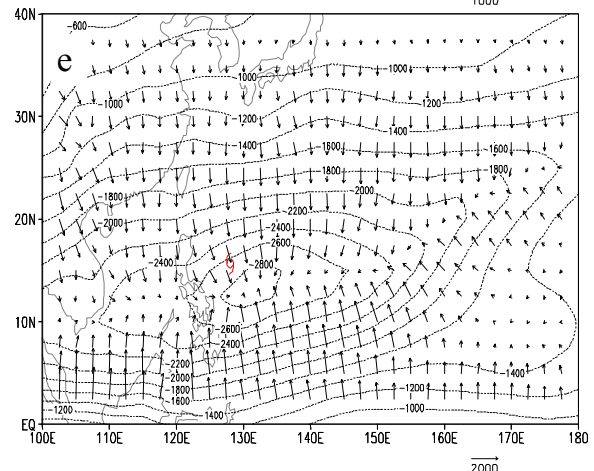
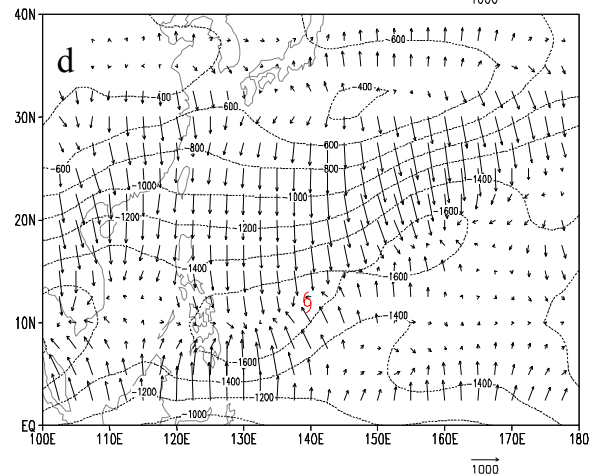
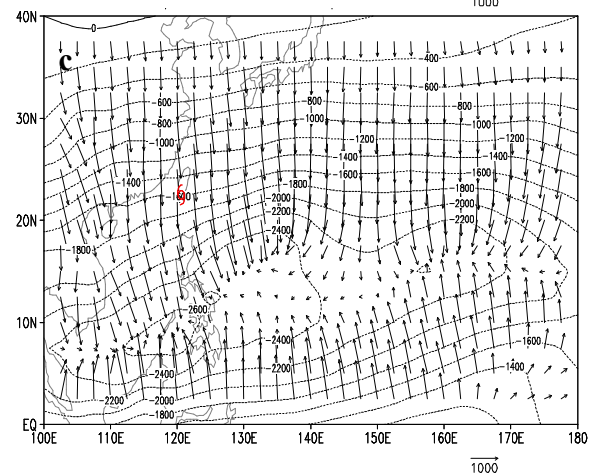
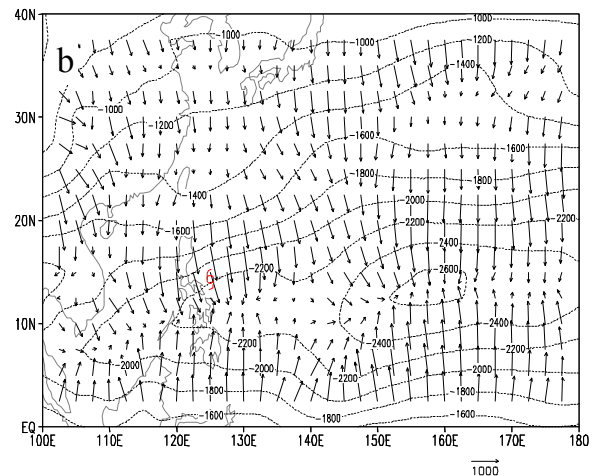
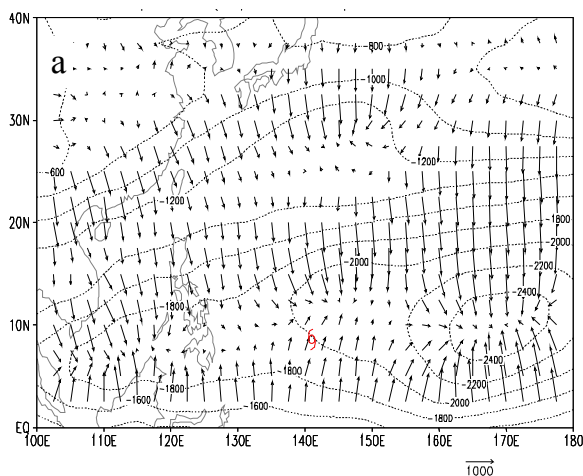
Water vapor is one of the most important factors in the genesis and development of a TC. After the outbreak of summer monsoon, the southwesterly over the Indian Ocean and SCS brings continuous, abundant water vapor and heat to the WNP and a monsoon trough is the most favorable system for TCs genesis. In wintertime, the direction of the wind changes, the southwesterly turns into a northeasterly, strong water vapor sources break off, and the Intertropical Convergence Zone (ITCZ) also retreats south to areas

near the Equator. How does the TC generate and develop and how does it move to the Chinese mainland north of 22°N? The source of water vapor and transportation channels under the circumstances are worth studying.

Similarly, physical variables such as water vapor at different stages of a TC, i.e., the generation, maturing, and weakening and dissipation, are calculated for analysis. In the process of Nanmadol, observational times at 0800 November 30, 0800 December 2, and 0800 December 4 are selected to represent the three stages while for the Irma, 0800 November 23, 0200 November 27, and 0800 December 2 are selected.

5.1 Characteristics of water vapor flux convergence

The velocity potential function of the whole-layer water vapor flux, which is vertically integrated from the ground surface to 300 hPa, is calculated, and the large-scale characteristics of moisture convergence during the processes of the TCs are explored. The potential function of water vapor flux reflects the water vapor flux passing through the isobar in transportation. While very small in the globe transportation, it plays an important part in the formation of sources and sinks of water vapor [12]. Figure 7 shows the velocity potential function and the divergent wind of the whole-layer water vapor flux in the period of formation, maturing, and dissipation in the two processes of TCs. Figure 8 gives the whole-layer vertical integration of water vapor flux divergence in the area within a $20^\circ \times 20^\circ$ range around the TC center for the illustration of the water vapor convergence in the TCs.



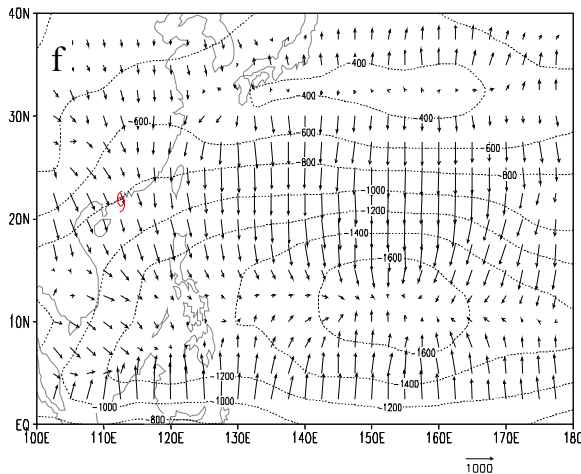


Fig.7 Whole-layer water vapor flux potential function (10^5 kg/s) and divergent wind ($\text{kg}/(\text{m} \cdot \text{s})$) for the phases of genesis, maturing, and dissipation of Nanmadol (a, b, c) and Irma (d, e, f).

It can be seen from Fig. 7a, 7b and 7c for the results of the Nanmadol process that there is an east-west water vapor flux convergence belt at 10°N in the WNP and the TC is located in a convergence circle 2000 units west of the largest convergence center when it first formed. There are two centers of water vapor

flux convergence at 160°E to 180° over the eastern WNP and 110°E to 120°E over the southern SCS in this convergence belt, respectively, of which the former was larger, reflecting major water vapor disturbance in the ITCZ. When the TC matured and moved to the northwest, there was also a convergence disturbance of water vapor flux in the vicinity of the TC, i.e., at 130°E east of the Philippines, while the convergence belt moved to the north, the convergence center shifted westward, and the values kept increasing till 2600 units; When the TC was making landfall, the center value of water vapor flux convergence remained at 2600 units and moved to the west over the Philippines. The TC was, however, located outside of the convergence belt, which was not conducive to the acquisition of a large amount of water vapor. From the whole-layer water vapor flux divergence fields (Figure 8a to 8c), it can be seen that in the TC generation and maturing stages, the area around it became a strong negative convergence zone; When it turned into a divergence zone of water vapor flux, there was already no continuous supplement of water vapor, causing the TC to weaken and decay.

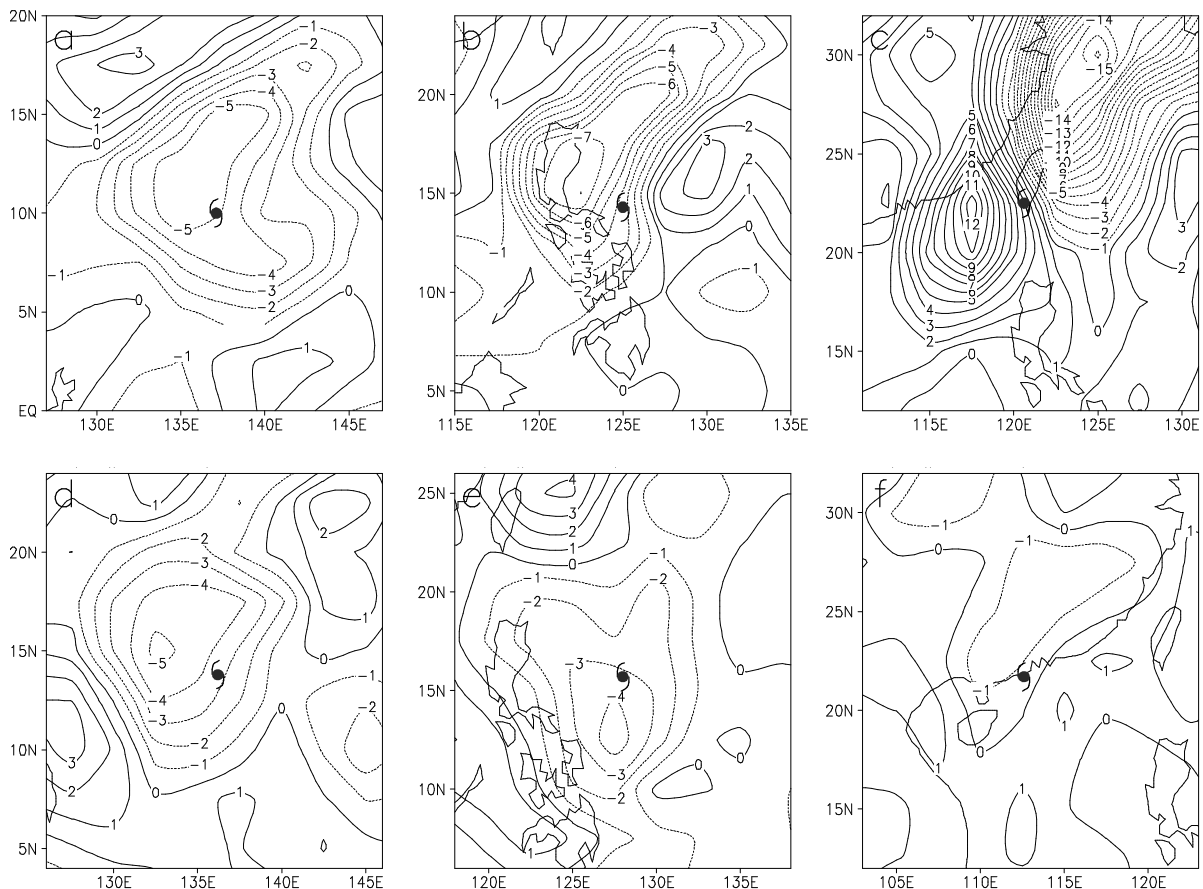


Fig.8 Whole-layer water vapor flux divergence for the phases of genesis, maturing, and dissipation of Nanmadol (a, b, c) and Irma (d, e, f). Units: $10^{-5} \text{ kg}/(\text{m}^2 \cdot \text{s})$. The typhoon symbol denotes the position of the TC center.

In the process of Irma (Figs. 7d to 7f), the east-west water vapor flux convergence belt was mainly located at 5°N to 20°N over the WNP when the TC was first generated and there were three convergence disturbance centers of water vapor flux in the vicinity of 100°E over the Bay of Bengal and in the vicinity of 130°E, 155°E over the WNP, respectively, of which Irma was located within the center in the middle. With the development of the TC, the WNP moisture convergence zone strengthened quickly. Before landfalling on the Philippines, the TC was always accompanied by a moisture convergence center, with the center value rising rapidly from the initial 1800 units to a maximum of 2800 units in this process. After landfalling on the Philippines, the TC gradually moved away from the moisture convergence center and the value of the water vapor flux convergence center reduced to the original 1600 units as the TC was generated. In the whole-layer water vapor flux divergence fields (Figs. 8d to 8f), the TC center was surrounded by a strong negative convergence zone in the periods of TC generation and maturing, and there was a lot of moisture convergence. When the water vapor convergence decreased within the area of TC, the TC weakened and decayed.

In a word, for a TC generated in the water vapor flux convergence belt, its formation and development cause the disturbance of water vapor convergence and strengthen the water vapor flux convergence, making the convergence belt strengthen and move northward together with the TC. When the TC is outside of the moisture zone, it cannot gain sufficient water vapor so that it gradually weakens and decays.

5.2 Characteristics of water vapor flux

Because the transportation and convergence of the water vapor flux mainly occur on the low levels, the 850-hPa stream and water vapor flux fields are selected for our research. The low-level jet is defined as an airflow at 850 hPa with wind speed ≥ 8 m/s, and the values of water vapor flux which are above $10 \text{ kg} / (\text{m} \cdot \text{hPa} \cdot \text{s})$ are called a large water vapor flux. When the low-level jet overlaps with the large water vapor flux, the former is called the water vapor transportation belt^[8]. With the southwest low-level jet being one of the major water vapor transportation belts for the TC in summertime^[4-7], what is the case for wintertime?

Here, the periods of TC genesis, maturing, and dissipation are still selected for analysis as in section 4. Figure 9a to 9c shows that the large water vapor flux values are mainly located over the north and south of the TC center or ahead of it during the genesis and maturing periods of Nanmadol. The maximum values

of the water vapor flux, which are larger than $45 \text{ kg} / (\text{m} \cdot \text{hPa} \cdot \text{s})$, are mainly located in the northern part of the TC center. Although the Nanmadol process has been accompanied by an easterly jet in the WNP, the large water vapor flux values associated with the jet are not located in the rear of the TC, but the front of it, i.e., the role of the water vapor transportation belt is not transporting the water vapor to the TC but channeling the water vapor of the TC to the mainland such that the water vapor convergence of the TC turns itself into a source of water vapor. It was not until the TC weakened and turned to make landfall that the easterly water vapor transportation belt behind the TC formed; but the water vapor was transported to lows on the westerlies as well rather than to the TC only. There were no belts of strong moisture transportation during the Nanmadol process; the TC got water vapor mainly from its own strong convergent updraft over the sea surface around it.

During the Irma process (Fig. 9d to 9f), the maximum water vapor fluxes were mainly located in the area north and south of the TC as those for Nanmadol. The low-level jet linking to the TC was a west-to-southwest flow near the Equator. This jet stream was especially evident in the early stages of TC formation and development, which extended all the way from 100°E to the TC center, and overlapped with the large water vapor flux area (Fig. 9d). There was also a water vapor transportation belt associated with the easterly jet over the northeastern part of the TC, indicating that the water vapor transportation of TC during the initial time relied mainly on the equatorial westerly and the subtropical high southeasterly, which were basically the same as in summer. However, these two water vapor belts weakened and broke off after the storm reached the typhoon intensity (Fig. 9e). As the TC moved northwest, the values of water vapor flux in the south of the TC gradually decreased and the westerly jet also weakened and did not link to the TC when it was about to make landfall. This shows that in the early stages of the TC formation, the equatorial westerly flow and the subtropical high southeasterly winds play an important role in the water vapor transportation for the TC, but did not persist very long. Like the case of Nanmadol, there is no strong moisture transportation belt during the Irma process.

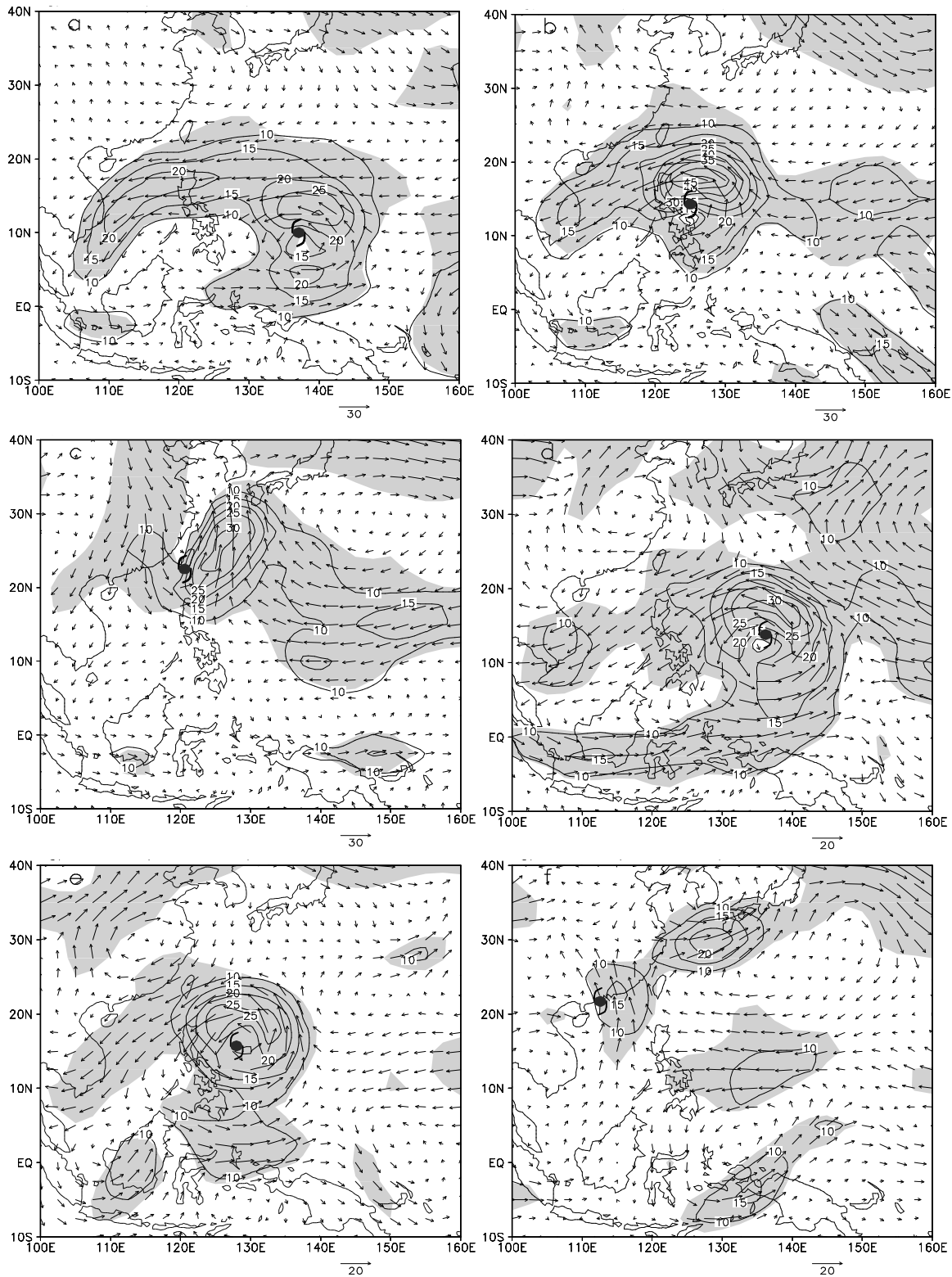


Fig.9 850-hPa water vapor flux (Contours $\geq 10 \text{ kg} / (\text{m} \cdot \text{hPa} \cdot \text{s})$; intervals: 5 units) and low-level jet (shades: wind speed $\geq 8 \text{ m/s}$) for the stages of genesis, maturing, and dissipation of Nanmadol (a, b, c) and Irma (d, e, f).

6 CONCLUSIONS

(1) During the two wintertime landfalling TC processes for China, a major East Asian trough steered the cold surge to the tropical ocean, which was

conductive to the development of tropical convection. When the sea-going cold high moved towards the TCs, the increasing pressure gradient outside of them contributed to the strengthening of the TCs. When the weak low-level cold air penetrated into the TCs, the

baroclinicity enhanced and cyclonic vorticity increased, thus increasing the TC intensity; when the strong cold air intruded into the mid- and low-levels of the TCs, the destruction of their warm core structure damaged and weakened the TCs.

(2) For the TCs generated in the disturbance of a moisture sink inside the water vapor flux convergence zone, its formation and development resulted in the disturbance of the water vapor convergence, strengthened the convergence of water vapor and convergence zone, making the latter move northward with the TCs. When the TCs broke away from the middle belt of moisture convergence and moisture convergence began to reduce, the TCs were weakened gradually until dissipation. Wintertime TCs, whose processes are not supplied with belts of strong water vapor, have obvious effect on the convergence of water vapor. Instead, the TCs depended on the equatorial westerly and the easterly winds south of the subtropical high for some amount of water vapor over a limited period of time. The TCs primarily relied on their own strong convergence updraft to gain the moisture needed from the sea surface around it after they reached the mature phase.

The above conclusions obtained through diagnostic analysis still needs further validation by numerical simulation experiments. The physical mechanisms of the effect of cold air and water vapor on the TC intensity still needs further study, and the abnormal climate background around the formation and development of wintertime TCs are also worth further exploration.

Acknowledgement: The present paper employs the NCEP reanalysis data provided by the NOAA/OAR/ESRL PSD, Boulder, Colorado, USA, from their website at <http://www.esrl.noaa.gov/psd/>.

REFERENCES:

- [1] LI Ying, CHEN Lian-shou, ZHANG Sheng-jun. Statistical characteristics of tropical cyclone making landfalls on China [J]. *J. Trop. Meteor.*, 2004, 20(1): 14-23. (in Chinese)
- [2] XIE Jiong-guang, JI Zhong-ping. Singular spectrum analysis for tropical cyclone landfalling in Guangdong [J]. *J. Trop. Meteor.*, 2003, 9(2): 201-207.
- [3] China Meteorological Administration. Tropical Cyclone Yearbook (2004) [M]. Beijing: China Meteorological Press, 2005. 131pp. (in Chinese)
- [4] CHEN Lian-shou, DING Yi-hui. Introduction to Western Pacific TCs [M]. Beijing: Science Press, 1979: 10-278. (in Chinese) editor
- [5] LIANG Li, WU Zhi-wei, YAN Guang-hua. The dynamic mechanism maintaining TC 9012 in active stage long after landfall [J]. *J. Trop. Meteor.*, 1995, 11(1): 26-34. (in Chinese)
- [6] YAN Guang-hua, LIN Zhong-ping, WU Zhi-wei. Analysis on satellite images and vertical structure characteristics of TC 9012 during its sustaining period after landfall [J]. *Taiwan Straits*, 1995, 14(2): 174-180. (in Chinese)
- [7] LI Ying, CHEN Lian-shou, WANG Ji-zhi. The diagnostic analysis on the characteristics of large scale circulation corresponding to the sustaining and decaying of tropical cyclone after its landfall [J]. *Acta Meteor. Sinica*, 2004, 62(2): 167-179. (in Chinese)
- [8] LI Ying, CHEN Lian-Shou, XU Xiang-De. Numerical Experiments of the Impact of Moisture Transportation on Sustaining of the Landfalling Tropical Cyclone and Precipitation [J]. *Chin. J. Atmos. Sci.*, 2005, 29(2): 91-98.
- [9] CHEN Ming, WU Kun-ti. Analysis of the Causes for the Abrupt Turning of TC Nanmadol's Path [J]. *J. South China Univ. of Trop. Agric.*, 2006, 12(3): 44-48. (in Chinese)
- [10] HE Jie-lin, GUAN Zhao-yong, NONG Meng-song. Preliminary study on structure of wintertime TC Nanmadol in 2004 [J]. *J. Trop. Meteor.*, 2008, 14(1): 69-72.
- [11] China Meteorological Administration. TC Yearbook (1974) [M]. Beijing: China Meteorological Press, 1975. 223pp. (in Chinese)
- [12] KALNAY E, KANAMITSU M, KISTLER R, et al. The NCEP/NCAR 40 year reanalysis project [J]. *Bull. Amer. Meteor. Soc.*, 1996, 77(3): 437-471.
- [13] DING Yi-hui. The diagnostic analysis methods for weather dynamics [M]. Beijing: Science Press, 1989: 174-199. (in Chinese)
- [14] DENG Guo, ZHOU Yu-shu, YU Zhan-jiang. Analysis of water vapor transportation in TC Dan (9914) [J]. *J. Trop. Meteor.*, 2005, 21(5): 535-538. (in Chinese)
- [15] CHANG C P, LAU K M. Short-Term Planetary-Scale Interactions over the Tropics and Midlatitudes during Northern Winter. Part I: Contrasts between active and inactive periods [J]. *Mon. Wea. Rev.*, 1982, 110(8): 933-946.
- [16] CHEANG B K. Synoptic features and structures of some Equatorial vortices over the South China Sea on the Malaysian region during winter monsoon, December 1973 [J]. *Pure Appl. Geophys.*, 1977, 115: 1303-1333.
- [17] SUN Bo-min, LI Chong-yin. The relationship between the disturbance of the East Asia trough and tropical convection [J]. *Chin. Sci. Bull.*, 1997, 42(5): 501-504. (in Chinese)
- [18] CHANG C P. Westward propagating cloud patterns in the tropical Pacific as seen from time-composite satellite photographs [J]. *J. Atmos. Sci.*, 1970, 27(1): 133-138.
- [19] WEBSTER P J. Response of the tropical atmosphere to local steady forcing [J]. *Mon. Wea. Rev.*, 1972, 100(7): 518-541.
- [20] CHANG C P, JOHNSON R H, KRIETE D C. Thermodynamic and circulation characteristics of winter monsoon tropical mesoscale convection [J]. *Mon. Wea. Rev.*, 1982, 110(12): 1898-1911.

Citation: HE Jie-lin, GUAN Zhao-yong, WAN Qi-lin et al. The role of cold air and characteristics of water vapor in both TCs Nanmadol (0428) and Irma (7427) making landfall on China in wintertime. *J. Trop. Meteor.*, 2010, 16(2): 160-170.